I&EC research
Industrial & Engineering Chemistry Research

Article

pubs.acs.org/IECR

Ultrasound-Assisted Antisolvent Crystallization of Benzoic Acid: Effect of Process Variables Supported by Theoretical Simulations

Kiran A. Ramisetty, Aniruddha B. Pandit, and Parag R. Gogate*

Chemical Engineering Department, Institute of Chemical Technology, Mumbai 40019, India

ABSTRACT: This work investigates the application of ultrasound for improving the antisolvent crystallization of benzoic acid. The main objective of applying ultrasound is to enhance the crystal productivity and modify the morphology as compared to the conventional stirred crystallizer. The effect of the sonication on the crystal size distribution and supersaturation ratio has been investigated. The effect of initial concentration of solvent and antisolvent addition rate on the crystal size and supersaturation ratio has also been studied under conventional mixing and ultrasound for effective comparison. The concentration of the solute in the liquid has been determined using HPLC at 228 nm wavelength so as to determine the supersaturation levels of solute. Dynamic growth kinetics of the crystallization process has been established by measuring the crystal size with respect to time. Dynamic metastable zone width was found by observing the formation of the crystal nuclei indicated by the liquid turning from transparent to slightly turbid. A decrease in the metastable zone width has been observed due to the application of ultrasound. The study of conventional crystallization has been conducted over varying impeller speeds of 400, 500, 600 rpm, and ultrasonic crystallization has been studied over different amplitudes of 40%, 50%, 60% amp using 750 W and 20 kHz frequency horn. Crystal size distribution has been observed to be wider in stirred crystallization process as compared to the ultrasound-assisted operation. Modeling of the process of antisolvent crystallization has been carried out using gProms PSE environment, and the comparison of the simulated results with the experimental results has been presented.

1. INTRODUCTION

Crystallization is an important process in the separation and purification cycle to produce a desired quality of materials in pharmaceutical, fine chemicals, and food industries. The subsequent processes such as filtration and drying are affected by the process of crystallization.[1,2]The important properties such as crystal size, shape, size distribution, and crystal habit are the specific target characteristics in the overall production process for the high value added products. This is especially important where the properties of the materials are significantly affected by the crystal size distribution and morphology. The main driving force for the crystallization is supersaturation. The formation of supersaturation in the case of cooling crystallization can be achieved by lowering the temperature of the preheated saturated solution, which decreases the solubility of solute in the solvent leading to the formation of the crystals. Cooling crystallization is not feasible for the compounds having weak or no dependency of the solubility on the temperatures.[3] Supersaturation can also be achieved by the evaporation of the solvent to increase the supersaturation, but this approach is not suitable for the crystallization of heat-sensitive materials, pharmaceutical products and explosives. Antisolvent crystallization is an alternative approach to overcome the difficulties in evaporative and cooling crystallization.[4,5] The formation of supersaturation in antisolvent crystallization is by the addition of an antisolvent in which the solute solubility should be very low or negligible. Antisolvent crystallization is an energy-saving process as compared to the cooling and evaporative crystallization. The major disadvantages of antisolvent crystallization are the chances of improper mixing of the antisolvent and the original solvent, coupled with the problems of solvent recovery process. The improper mixing of antisolvent can result in the undesired spontaneous nucleation and highly localized supersaturation leading to agglomerated crystals[6] having a large crystal size.

Antisolvent crystallization is mainly employed for the crystallization of organic compounds from water-soluble inorganic solvents and vice versa. Antisolvent crystallization is also called as drowning out crystallization in which two solvents are used to separate the solute preferentially. One solvent should have the property of high solubility toward the target solute, and another solvent (antisolvent) should have very low or no solubility toward the solute. Addition of antisolvent to the saturated solution of solute and solvent initially can increase the solubility, but continuous addition finally reduces the solubility of the solvent due to the highly miscible nature of the antisolvent and solvent, which decreases the amount of solvent available for the solute to be in a soluble state. This observation of decrease in solubility with addition rate of antisolvent can be observed in the case of paracetamol in a methanol−water mixture.[7] As the antisolvent addition decreases the solubility of the solute, the solute tries to be in a stable state by reaching a point of nucleation leading to the onset of crystallization. The metastable zone width can be determined as the amount of antisolvent required to form the nucleation from its saturation state. This can also be determined in terms of the time taken for the nucleation from its saturation state, which is called as the induction time. The selection of antisolvent plays an important role in precipitating the solute from the solution effectively. In recent studies, gas is also used as an antisolvent,

Received: July 11, 2013
Revised: October 15, 2013
Accepted: November 11, 2013
Published: November 11, 2013

dx.doi.org/10.1021/ie402203k | *Ind. Eng. Chem. Res.* 2013, 52, 17573−17582

reducing the downstream processing of separating the solvent and antisolvent. However, it may increase the capital cost due to the requirement of high pressure equipments.[8] Metastable zone width plays an important role in the process of crystallization. For antisolvent crystallization, the MSZW can be described as the ratio of antisolvent to solvent or the amount of antisolvent added from saturation point to the point of the appearance of nucleation. The MSZW rises above the solubility curve at which spontaneous nucleation occurs in supersaturated liquid.

The process of combined cooling and antisolvent crystallization for specific compounds is another emerging technique to achieve the desired supersaturation and crystal size distribution of crystals. Nagy et al.[9] hase developed the strategies for the combined antisolvent cooling crystallization of lovastatin in a batch crystallizer. Lindenberg et al.[10] have also optimized the process of combined cooling antisolvent crystallization.

The influence of ultrasonic waves on the crystallization process in terms of nucleation of crystals in different types such as cooling, antisolvent, and evaporative crystallization can be significant in controlling the final product characteristics. Applying the ultrasonication in the supersaturated solution can cause a primary nucleation.[11] As the ultrasonic waves propagate in the supersaturated solution, it induces the phenomena of transient cavitation, which creates vapor cavity bubbles in successive cycles of compression and rarefaction of the sound waves.[12] In rarefaction, there is a formation of gas/vapor cavity bubble, which collapses in the subsequent compression, creating a condition of high temperature and pressure and also decreasing the supersaturation of the liquid, at the same time increasing the metastable zone width for the formation of nuclei. The liquid gets highly supersaturated immediately (due to solvent vaporization/quenching) and results in nucleation earlier than in the conventional process, leading to reduced metastable zone width. Other postulate suggests that the rarefaction part of ultrasonic waves can vaporize the liquid in the vicinity of cavity so that the liquid experiences highly rapid local cooling (quenching) and gives significant supersaturation to create nucleation in liquid.[13,14] It has been assumed that the number of nuclei formed in the liquid is equal to the number of cavitation events.[15] So each nucleus grows as a crystal, which will result in more number of crystals due to the application of ultrasound resulting in narrow size distribution in the ultrasound-assisted crystallization. Another main advantage of ultrasound-assisted crystallization can be reduction in agglomeration of crystals.[16] Ultrasound-assisted antisolvent crystallization offers an effective alternative to the process of milling and micronization to prepare the inhalation drugs for respiratory disorders with significantly improved particle morphology, size, crystallinity, and stability.[17]

The present work deals with an approach for finding the crystal growth and nucleation rates of ultrasound-induced crystallization of benzoic acid based on the sampling of the crystals for their characterization with respect to time. Modeling studies have been incorporated to understand the basic principles of kinetics and modeling parameters for the process of antisolvent crystallization. Ultrasonic crystallization of benzoic acid to study the effect on morphology and size has not been reported in the literature, and hence this also forms a novel objective of the work.

Process modeling can be a prominent technique to reduce the operational cost based on the developed understanding and optimization of crystallization in industry. gProms is the software that can accomplish the solution of the process modeling equations of crystallization to simulate the process. In the present study, modeling of crystallization is also attempted considering the basic equations of population balance and mass balance in crystallization using gProms. The modeling of mass balance in crystallization should be combined with the population balance equation, because it is a particulate system with combined process of crystal nucleation and growth. Theoretical explanation and derivation of population balance equation can be referred to the earlier work reported in the literature.[1] In antisolvent crystallization, population balance equation involves the terms as change in crystal number density with time, change in crystal number density with growth, change in crystal number density with change in the solution/slurry volume due to the addition of antisolvent, nucleation rate, agglomeration, and breakage. In the present study, agglomeration and breakage terms are neglected to simplify the process of simulation. It is also important to note here that, depending on the experimental conditions such as method of addition of the antisolvent and initial concentration of the solute, the modeling process may vary and needs to be modified incorporating appropriate equations.

2. MATERIALS AND METHODS

2.1. Materials. Benzoic acid, ethanol, and distilled water were used as the solute, solvent, and antisolvent, respectively, to study the effect of sonication on the antisolvent crystallization. Benzoic acid and absolute ethanol (99.9%) were obtained from S.D. Fine Chem., Ltd., Mumbai. Distilled water has been used as an antisolvent, and dropwise addition is done using a peristaltic pump obtained from Enertech Pvt. Ltd., Mumbai. Sonics VC 750 (maximum power is 750 W) ultrasonic processor operating at 20 kHz frequency has been used to study the effect of sonication on the process of crystallization. For maintaining the temperature of the mother liquor at 30 °C, a temperature controlled cooling system has been used with silicon oil as a circulating liquid through the jacketed glass reactor. For comparing the ultrasonic sonocrystallization with conventional crystallization, a pitched blade impeller (REMI Motors Pvt. Ltd., Mumbai) has also been used instead of an ultrasonic horn to study the conventional stirring-based crystallization process. A magnetic stirrer has been used in the case of ultrasonic crystallization for moderate mixing of the components. Samples of crystals and slurry have been collected using a micro pipette and placed in micro centrifuge tips for the filtration, drying, and analysis of the supernatant solution. Concentration of benzoic acid has been measured using an Agilent HPLC C18 column (Agilent Technologies Pvt. Ltd.). Leica microscope with camera has been used for the measurements of the crystal size of benzoic acid. ImageJ and Fiji image processing software were used to analyze the obtained images and obtain the crystal size and the distribution.

2.2. Experimental Methodology. A schematic representation of the experimental setup is shown in Figure 1. Initially 32 g of benzoic acid was dissolved in 100 mL of absolute ethanol, corresponding to the concentration of 0.4 kg of benzoic acid per kg of solvent. This solution is mixed using a stirrer to prepare an unsaturated solution of benzoic acid−ethanol at room temperature, and then transferred to a three-neck baffled jacketed reactor. The inlet and outlet of jacket of the reactor are connected to the controlled cooling system for circulation of the silicon oil. The temperature of the solution

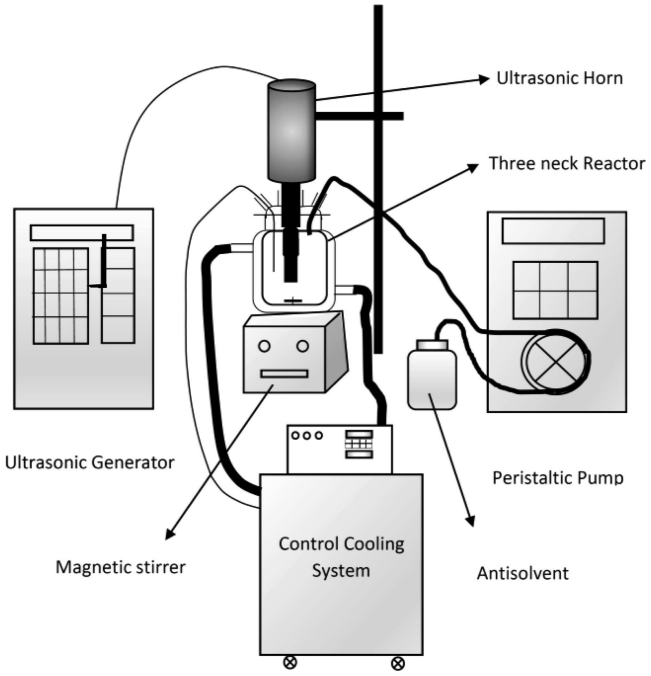

Figure 1. Schematic representation of the experimental setup of ultrasonic antisolvent crystallization.

mixture is controlled at 30 °C. Antisolvent (filtered distilled water) has been added using a peristaltic pump with varying flow rates over the range of 0.018−0.1 mL/s. Drop by drop addition of antisolvent changes the solution solubility from the unsaturation to the saturation stage. Any addition beyond the saturation level is expected to give crystals. A continuous application of ultrasound using ultrasonic horn to the liquid has been achieved to study the effect of sonication on the meta stable zone width, nucleation rate, and the growth rate of benzoic acid crystals. Increase in the temperature of the solution due to the application of ultrasound has been counteracted with the controlled cooling system. Care has been taken to start the addition of antisolvent after the solution temperature stabilizes at 30 °C. Sonication has been replaced with the stirring to study the conventional crystallization and its comparison with the sonication-based approach. The solubility curve of benzoic acid showing the variation of solubility with antisolvent and solvent ratio is shown in Figure 2. An excess amount of benzoic acid has been added to the mixture of ethanol and water with ratios from 0 to 1 at 30 °C of temperature. Undissolved benzoic acid has been filtered to confirm the solubility of benzoic acid in ethanol−water mixture of varying compositions.

With further increase in the addition of antisolvent, the solution turns from the saturation state to the supersaturation state, and the point in the metastable zone width is reached where formation of nuclei has been observed. MSZW has been measured using the continuous image capturing of the solution, for observing the turning point from the clear transparent liquid to turbid liquid. This has been achieved by continuous addition of antisolvent until the liquid attains the dynamic MSZW. In the case of ultrasonic crystallization, if there is no agitation in the solution, the formed crystals are stuck to the surface of the glass jacketed reactor as the outer liquid temperature is lower as compared to the inner liquid temperature, and then there is a chance of formation of additional nuclei. This has been avoided

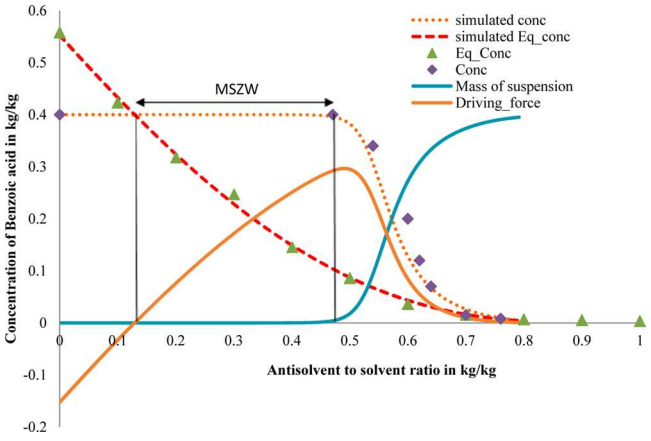

Figure 2. Benzoic acid solubility curve, mass of crystals, and supersaturation as driving force with the ratio of antisolvent to solvent.

by a continuous and adequate stirring of the solution using a magnetic stirrer. It is important to note here that this agitation due to the magnetic stirrer may affect the attrition of the formed crystals, but adequate stirring was essential to keep the crystals in motion, avoiding possible sticking to the reactor wall where there is a chance of formation of secondary nucleation on the surface of formed crystals and agglomeration of the crystals. Samples were taken immediately after the formation of crystals using micro pipette. The residual solution is a clear solution of benzoic acid, ethanol, and water mixture. These solutions were kept in airtight micro centrifuge tubes for further analysis for finding the concentration of benzoic acid using HPLC. Variable wavelength detector (VWD) has been used at wavelength of 228 nm, and HPLC grade methanol has been used as the mobile phase. The crystals were transferred on a glass plate to measure the crystal size using a microscope at 4× optical zoom. About 100 photographs were taken for each sample to analyze a number of crystals to measure the mean size in terms of Sauter mean diameter. An ImageJ macro program has been used to measure the particles in all of the photographs using an optimized approach as described in our earlier work.[18]

3. MATHEMATICAL MODELING

A model for the antisolvent crystallization system of benzoic acid, ethanol, and water has been developed using population balance equation model and the gPROMS PSE environment. Crystal growth rate and nucleation rate were calculated from the experimental results to incorporate the values of growth and nucleation coefficients in the simulation. All of the parameters and variables are considered on a mass basis. The population balance model for the antisolvent crystallization was adopted from the literature[19,20] with an assumption of no breakage and no agglomeration in the process. The equation is given below:

$$\frac{\mathrm{d}n(L)}{\mathrm{d}t} + G\frac{\partial n(L)}{\partial L} + \frac{n(L)}{m_{\mathrm{T}}}\frac{\mathrm{d}m_{\mathrm{T}}}{\mathrm{d}t} = B \quad (1)$$

Here, $n(L)$ is the population density in number/m^3, G is the crystal growth in m/s, L is the characteristic length in m, m_{T} is the total mass of the solution in kg, and B is the nucleation rate in number/m^3/s. The term $\mathrm{d}n(L)/\mathrm{d}t$ describes the change in crystal number density with respect to time, whereas the term $G(\partial n(L)/\partial L)$ describes the change in crystal number density due to the growth in crystal size between L and $\mathrm{d}L$. The

dx.doi.org/10.1021/ie402203k | Ind. Eng. Chem. Res. 2013, 52, 17573−17582

expression $(n(L)/m_T)(dm_T/dt)$ takes into account the changes in solid mass with respect to time as it increases in antisolvent crystallization due to the continuous addition of antisolvent.

The basic mass balance equation for the modeling of antisolvent crystallization was adopted from Noweeetal[21] and is given below:

$$\frac{dm_T}{dt} = \frac{dm_s}{dt} + \frac{dm_l}{dt} \tag{2}$$

The change in total mass (m_T) of solution with time has been divided into two parts and is equal to the increase in mass of liquid content (m_l) due to addition of antisolvent and changes in the mass of crystals (m_s), which are formed due to the formation of nuclei and subsequent growth.

The change in liquid mass is determined as the summation of the initial solvent mass and the quantum of antisolvent added during the process.

$$m_l = m_{solvent} + Qt \tag{3}$$

where m_l is the mass of liquid phase in the solution, $m_{solvent}$ is the mass of initial solvent added and dissolved benzoic acid, Q is the antisolvent flow rate, and t is the time.

The change in solid mass (m_s) has been determined as the mass of the crystals formed in the crystallizer due to nucleation and/or growth.

$$m_s = \rho_c k_v \int n(L)L^3\, dL \tag{4}$$

ρ_c is the density of benzoic acid crystal (1316 kg/m^3),[22] and k_v is the shape factor.

Mass balance of the solute indicates that the rate of decrease in the concentration of the solute in liquid is equal to the rate of formation of the solid crystals in the solution. Considering this, we can write the following balance:

$$\frac{dC}{dt} + \frac{dM}{dt} = 0 \tag{5}$$

where C is the concentration of the solute in kg//kg of solvent, and M is the magma density in kg/kg of solution. The rate of formation of crystals can be determined using the following equation:

$$\frac{dC}{dt} = -3\rho_c G k_v \int_{\infty}^{0} n(L)L^2\, dL \tag{6}$$

In the above equation, growth rate G (m/s) is given by the following equation:

$$G = k_g\left(\frac{(C - C^*)}{C^*}\right)^g \tag{7}$$

where k_g is the growth coefficient, g is the order of the growth, C is the concentration of solute in the solution and C* is the saturated concentration of solute in the mixture.

Nucleation rate (B) of the crystals is given as:[23]

$$B = k_b(1 + i^*M)\left(\frac{(C - C^*)}{C^*}\right)^b \tag{8}$$

where k_b is the nucleation coefficient, and b is the order of the nucleation. Saturated concentration (C^*) of the solute has been found experimentally at 30 °C, and an empirical equation can be fitted as shown in Figure 2.

$$C^* = -0.4985x^4 + 0.912x^3 + 0.2724x^2 - 1.2327x + 0.5526 \tag{9}$$

where x is the fraction of antisolvent mass in the total mass of liquid, and can be expressed as:

$$x = \frac{Qt}{(m_{solvent} + Qt)} \tag{10}$$

All of the equations were used in gProms modeling environment to simulate the antisolvent crystallization with variables as C^*, σ, C, ΔC, M, $n(L)$, G, B, m_T, m_L, m_S and the initial known parameters as Q, ρ_c, k_v, k_g, k_b, g, b, $m_{solvent}$. The boundary condition used in the simulation process is that population density at the formation of nucleation assuming the nuclei size zero is equal to the ratio of nucleation rate and growth rate.

$$n(0, t) = \frac{B}{G} \tag{11}$$

Initial conditions for the process of simulation were used as follows: at time $t = 0$, the change in the mass of the generated crystals is $dM/dt = 0$, the total mass of liquid is the mass of the liquid phase as there is no formation of crystals $(m_T = m_{solvent})$, and the population density of the crystals is zero $(n(L,0) = 0)$.

4. RESULTS AND DISCUSSION

4.1. Growth and Nucleation Kinetics. Experiments were conducted using both processes of conventional and ultrasound-assisted crystallization to compare the effect of sonication on the growth and nucleation coefficients. The nucleation and growth are the sequential phenomena, as the formation of new nuclei due to the addition of antisolvent in the dynamic antisolvent crystallization is followed by the growth with the time. At any time of crystallization, there will be a presence of small nuclei crystals as well as completely grown crystals as the process of nucleation is not controlled. So the mean crystal size has been considered for finding the crystal growth rate. Crystal growth kinetics for antisolvent crystallization of benzoic acid can be established using the following equation:

$$G = \frac{dL}{dt} \tag{12}$$

The variation in the crystal size with respect to time has been established by sampling the crystals at a particular time of crystallization. After nucleation, crystals were taken out and filtered using vacuum filtration to separate the crystals and clear solution. However, the process was not simple as ethanol is a volatile liquid, and it can immediately escape from the sample when it is poured on the Whatman filter paper under the action of vacuum. This evaporation rate of ethanol depends on the concentration of ethanol in the solution, and as the antisolvent amount increases (because water is the antisolvent), this contribution of evaporation would decrease. If the purpose is only to collect the crystals, it would not be that important to consider the problem of evaporation. On the basis of these observations, it has been decided to filter the sample on filter paper without using vacuum. Because of lower porosity of the Whatman filter paper, liquid filtered out slowly, and it results in an increase in the crystal size on the filter paper because of the low boiling point of ethanol. These newly formed crystals agglomerated on the surface of filter paper. So some amount of

dx.doi.org/10.1021/ie402203k | Ind. Eng. Chem. Res. 2013, 52, 17573−17582

the mother liquor was taken out immediately and absorbed on the surface of 4-fold tissue paper, such that the paper is completely saturated and subsequently only crystals are accumulated on the surface of the paper. Sample was also kept in a micro centrifuge tube for about 1 min to sediment the crystals, and clear solution was taken out and injection filtered into another vial for further analysis using HPLC for finding the concentration of dissolved benzoic acid. The collected crystals were observed under microscope. A graph between the crystallization time and crystal size has been shown in Figure 3 for the ultrasonic crystallization at antisolvent flow rate of

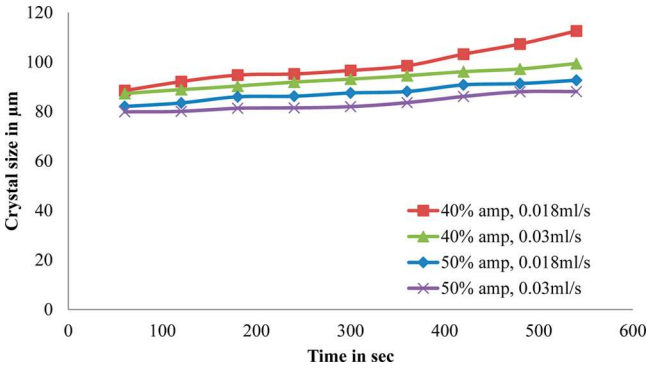

Figure 3. Change in crystal size with respect to time to find the crystal growth.

0.018 and 0.037 mL/s with 40% and 50% amp of sonication. Growth constant k_g and growth order g were found by using change in supersaturation ratio ($\sigma = (C - C^*)/(C^*)$) of the solute with respect to time in the solution and corresponding growth rate ($G = dL/dt$). These values were incorporated into eq 7 to get the slope and intercept of graph between logarithmic values of growth rate and supersaturation ratio as shown in Figure 4. Nucleation rate (B) has been found using eq

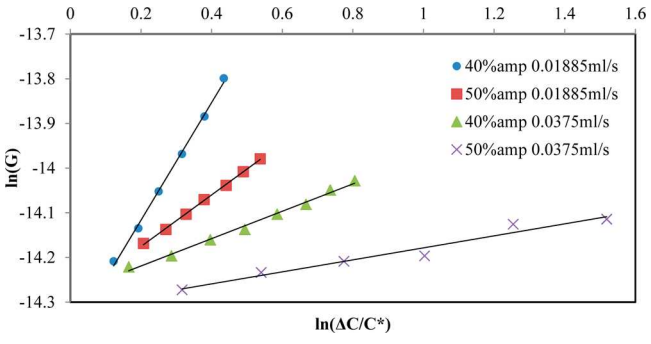

Figure 4. Logarithmic graph between growth rate and supersaturation ratio.

8. Number of nuclei has been found by taking the ratio of amount of solute crystallized out immediately after nucleation to the mass of single crystal, which gives the number of crystals after nucleation. These parameters were fed in the simulation program in gProms to predict the remaining variables such as suspension mass M, population density $n(L,t)$, and concentration of solute C.

4.2. Metastable Zone Width (MSZW). The obtained experimental results for MSZW have been compared to gProms simulated results predicted by the software on the basis of the pattern of decrease in the concentration with respect to the antisolvent to solvent ratio. From eq 5, it can be observed that the rate of decrease in the concentration equals the increase in the crystal deposition rate. This concentration change occurs as the crystal deposition starts, and hence both of these parameters are dependent on each other as the process continues. Nucleation rate (k_b), growth rate coefficients (k_g), and driving force (ΔC) are the key process variables for obtaining the MSZW using the simulations. In the present work, for the simulation for MSZW, any parameters related to the ultrasonic mixing (frequency or power of ultrasonic irradiations) have not been included in the simulation. The experimental values obtained from the data sets such as k_b, k_g, and ΔC are provided to the simulation program.

The experimental study of MSZW in the antisolvent conventional crystallization and ultrasonic crystallization has been performed with varying flow rates of antisolvent and power dissipation (only in the case of sonocrystallization). Figure 5 represents the change in metastable zone width

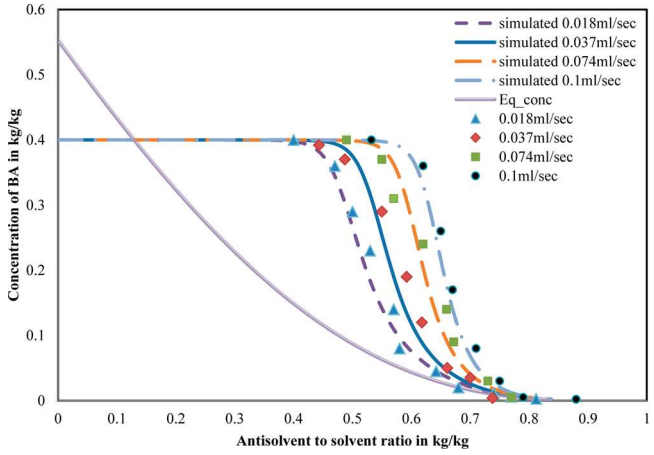

Figure 5. Prediction of metastable zone width with addition rate of antisolvent at 400 rpm.

obtained using experimental analysis and simulations with respect to the antisolvent addition rate for conventional crystallization at 400 rpm. The simulation results show a good match with the experimental results validating the model and the solution methodology. Simulation of metastable zone width is represented in the corresponding antisolvent to solvent ratio rather than the time of crystallization as the antisolvent rate is the main cause for the variation of metastable zone width. In a conventional stirring process, the MSZW is mainly affected by the mixing of antisolvent and solvent by the stirrer. If the addition of antisolvent is on the surface of the liquid, improper mixing will create local supersaturation leading to the formation of earlier unstable nucleation and hence decreased MSZW. Crystals formed due to this earlier supersaturation in conventional crystallization operated with improper mixing are random, irregular in shape, and unevenly distributed. To overcome this, antisolvent addition has been tried under the impeller to give proper mixing of antisolvent and solvent. The tip of the pipe has been modified to have a cone shape by attaching a micro centrifuge tip to reduce the exit diameter of pipe, in which the liquid will be delivered with high velocity, and this will not allow the solvent to rise into the pipe used for introducing the antisolvent and avoiding the plugging of the pipe. Increase in the MSZW has been observed with the addition of antisolvent under the stirrer than on the surface of

dx.doi.org/10.1021/ie402203k | Ind. Eng. Chem. Res. 2013, 52, 17573−17582

the solution due to the elimination of the formation of earlier nucleation due to a high rate of mixing and produced slightly bigger crystals when compared to the addition of the antisolvent on the surface of the solution. These studies clearly confirm the dependence of MSZW and crystal size on the level of mixing in the crystallizer.

In the case of ultrasonic crystallization, as shown in the Figure 6, the metastable zone width decreased significantly as

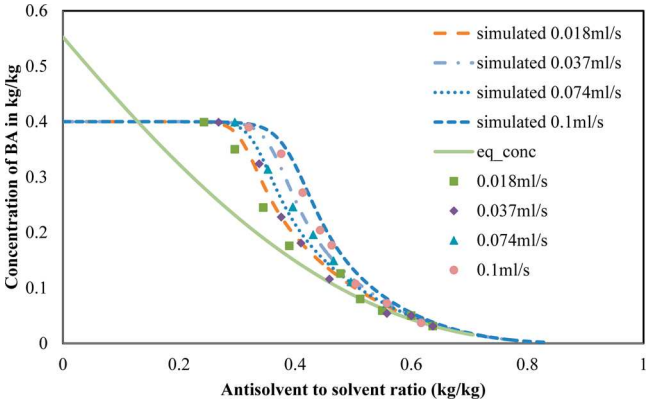

Figure 6. Prediction of metastable zone width with antisolvent addition rate at 40% amp of ultrasound.

compared to the conventional crystallization (at similar antisolvent addition), but the simulation results for the ultrasonication case do not match with the experimental values. The observed mixing pattern of liquid in the ultrasound-assisted setup is like spreading from the surface of probe to liquid volume in conical shape. This pattern also depends on the efficiency of energy transfer, intensity of ultrasonicator, frequency, and the volume of the liquid. Mixing in the case of ultrasonic crystallization is better as compared to stirring and the addition of antisolvent on the surface of liquid created local supersaturation with narrow MSZW, and hence the formed crystals due to this earlier nucleation are lower in size, regular, and uniform. This is mainly due to the phenomena of cavitation and resultant micro mixing of solute.[24] On comparison of the results of conventional crystallization with ultrasonic-induced crystallization, a decrease in the metastable zone width has been observed to be more in ultrasonic crystallization. Creation of number of nuclei due to cavitation has more effect on the metastable zone width in the presence of sonication, which can reduce the operating cost of the crystallization by reducing the required quantum of antisolvent and also the separation load of this antisolvent.

4.3. Effect of Initial Concentration of Benzoic Acid. The effect of initial concentration of the benzoic acid on the metastable zone width and the induction time has been investigated with varying concentrations of benzoic acid as 0.40, 0.44, 0.48, 0.52 kg/kg of ethanol, at constant ultrasonic power of 40% amp, and constant flow rate of antisolvent addition as 0.018 mL/s with temperature being maintained at 30 °C. A decrease in metastable zone width has been observed with an increase in the initial concentration of benzoic acid. There is a rapid reduction in the concentration of benzoic acid as the metastable zone width decreased with an increase in the initial concentration of benzoic acid. This is expected as with an increase in the initial concentration, the solution becomes more supersaturated, which is directly related to the growth and nucleation rate. It has been observed that there is an increase in the number of crystals with an increase in the initial concentration due to the high nucleation rate of crystals. A decrease in crystal size has been also observed with an increase in the initial concentration due to high nucleation rate.[7] Simulation of the process has also shown that the same results of decrease in metastable zone width with an increase in the initial concentration of benzoic acid are obtained as shown in Figure 7.

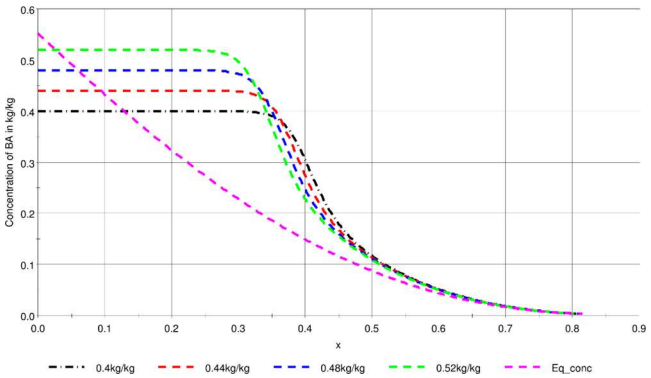

Figure 7. Effect of initial concentration on the metastable zone width.

4.4. Effect of Agitation Rate on the Crystal Size. Crystal size distribution is greatly influenced by the agitation rate, and hence the effect of agitation has been studied using a pitched 6-bladed impeller having a diameter of 30 mm at the rotational speed of 400, 600, and 800 rpm. As soon as the droplet of antisolvent is added to the solution on the surface, the precipitation of solute benzoic acid is expected to start. If sufficient agitation rate is applied, the precipitated solute again dissolves in the liquid due to the lower supersaturation. As the supersaturation increases, if the agitation rate is not sufficient to mix the antisolvent and solvent, chances of formation of conditions of local high supersaturation[25,26] can lead to instant nucleation. There is an increase in crystal size and shifting of the crystal size distribution (CSD) toward higher size with increasing agitation rates as shown in Figure 8. These

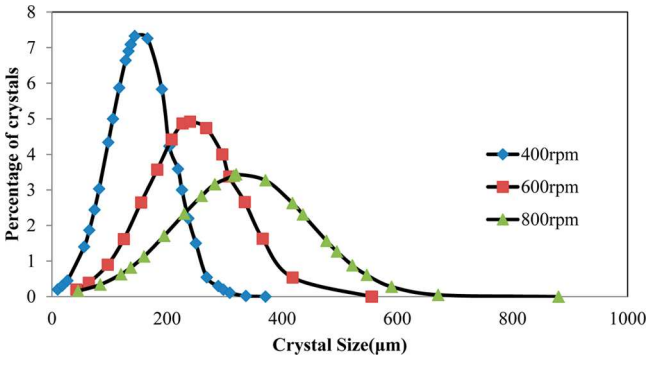

Figure 8. Effect of agitation rate on the crystal size of benzoic acid at a flow rate of 0.018 mL/s.

distribution curves are plotted by fitting the data obtained from the ImageJ processing to normal distribution with Sauter mean diameter ($L_{32} = (\sum L^3)/(\sum L^2)$) as the mean. The Sauter mean diameters are 140 , 250, and 340 μm for the corresponding agitation rates of 400, 600, and 800 rpm at a constant temperature of 30 °C, initial concentration of 0.4 kg/kg, and antisolvent addition rate of 0.1 mL/s. The observed

trends can be attributed to the fact that as the agitation rate increases, the degree of uniform mixing of antisolvent in the liquid also increases along with an enhancement in the mass transfer coeffient.[27] This increase in mass transfer at liquid solid interface results in an increase in the crystal growth rate and hence the crystal size. Change in crystal size with respect to time was also calculated to find the crystal growth rates at different agitation rates. It has been reported and also observed experimentally in the current work that, at higher addition rate of antisolvent and lower agitation speed, local supersaturation levels[19] increase significantly. The observed trends of behavior of increase in crystal size with agitation rate are supported by the results of reactive crystallization of benzoic acid.[28] However, in contrast to the current experimental observation, crystal size in antisolvent crystallization has been reported to decrease with increasing agitation in the case of carbamazepine crystallization from organic solvents,[29] and in another work it has been reported that there is no effect of agitation rate on crystal size in an antisolvent crystallization of ethylcellulose.[30] Thus, it is very important to establish the effect of agitation for the specific compound such as benzoic acid, and hence the present work is significant.

The population density of the crystals was predicted using the gProms simulation. The change in crystal population density with respect to the time of crystallization has been given in Figure 9. As the time of crystallization increases, the population density increases, and the CSD becomes broader and is shifted toward the higher size (Table 1). The predicted final crystal size distribution is found to match with the experimental results as seen in Figure 9.

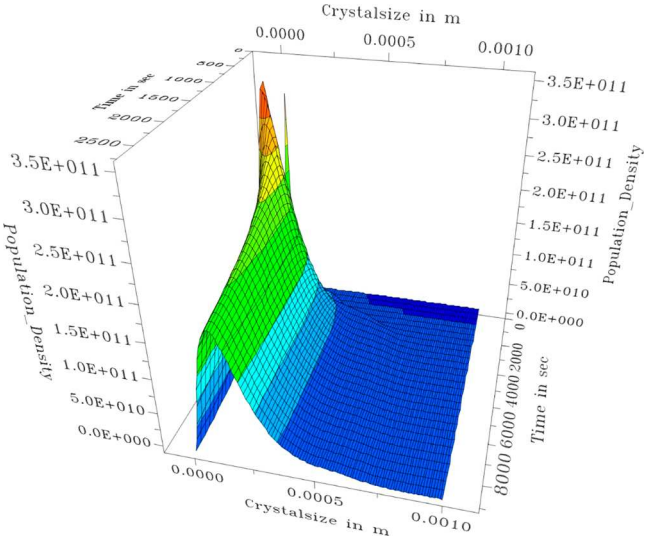

Figure 9. The prediction of population density of benzoic acid crystals at 600 rpm and 0.018 mL/s at $k_g = 2.6 \times 10^{-6}$, $k_b = 3.2 \times 10^7$.

4.5. Effect of Ultrasonic Power on Crystallization. There have not been many studies dealing with understanding the effect of ultrasonication on the crystallization of benzoic acid. The effect of ultrasonication on the crystal size of the benzoic acid and morphology of crystal was concentrated in this study. From the conventional crystallization study, it was found that the crystal shape is rectangular or in the form of hexagonal plates, but rarely are needle shape crystals observed.[31] The careful observation of the surface of these crystals confirms the agglomeration or formation of small crystals with irregular structure as shown in Figure 10a. Yet when the crystallization was conducted in the presence of ultrasound, it was observed that there is production of crystals with the same morphology of benzoic acid with clear edge appearing as hexagonal structure, but considerable reduction in size has been observed as compared to the conventional stirring approach. Very clear surface of crystals has been observed with low size and no agglomeration as compared to the conventional stirring-based crystallization as shown in Figure 10b.

Experiments were also performed under varying power dissipation levels by changing the percentage amplitude as 40%, 50%, 60%. The power delivered to the system was 66, 102, 145 W, respectively, under these amplitudes. Ultrasonication increases the liquid temperature to 50 °C within 15 min, which increases the induction time. To avoid this effect, controlled cooling system has been used to maintain the temperature at the set point of 30 °C. Because of the phenomena of acoustic cavitation, earlier nucleation and formation of very small crystals has been observed as depicted in Figure 10 at 40% amp of ultrasound. These crystals were sampled out, and crystal size distribution was measured at specific intervals of time for finding the growth rates as shown in Figure 11. The mean crystal size was observed to be about 88−104 μm between the time intervals of 2−10 min time. This decrease in crystal size due to application of ultrasound is also confirmed by similar reports in the case of carbamazepine crystallization with water as antisolvent.[32] At particular addition rate of antisolvent, the crystal size obtained with higher power of ultrasound is low with narrow distribution when compared to lower power of ultrasound as shown in Figure 11. The number of crystals formed was observed to be increased due to introduction of ultrasound and also the size reduced. The observed results can be attributed to the fact that use of ultrasound enhances the nucleation rate significantly, and hence the number of nuclei formed is increased. As soon as the antisolvent is added to the solution, its distribution into the

Table 1. Experimental Parameters Used in Simulation Process To Find the Population Density of the Crystals

ultrasonic amplitude	initial concentration (kg/kg)	flow rate (mL/s)	K_g	g	K_b	b
40%	0.4	0.018	5.6×10^{-8}	2.5	1.5×10^9	1.2
40%	0.4	0.037	4.2×10^{-8}	2.1	1.8×10^9	1.5
50%	0.4	0.018	3.5×10^{-8}	2.3	1.9×10^9	1.7
50%	0.4	0.037	3×10^{-8}	1.8	2×10^9	2.1
mechanical agitation speed (rpm)	initial concentration (kg/kg)	flow rate (mL/s)	K_g	g	K_b	b
400	0.4	0.018	1.5×10^{-6}	3.1	1.2×10^7	1.6
600	0.4	0.018	2.6×10^{-6}	3.5	3.2×10^7	1.9
800	0.4	0.018	3.2×10^{-6}	3.8	3.6×10^7	2.3

dx.doi.org/10.1021/ie402203k | Ind. Eng. Chem. Res. 2013, 52, 17573−17582

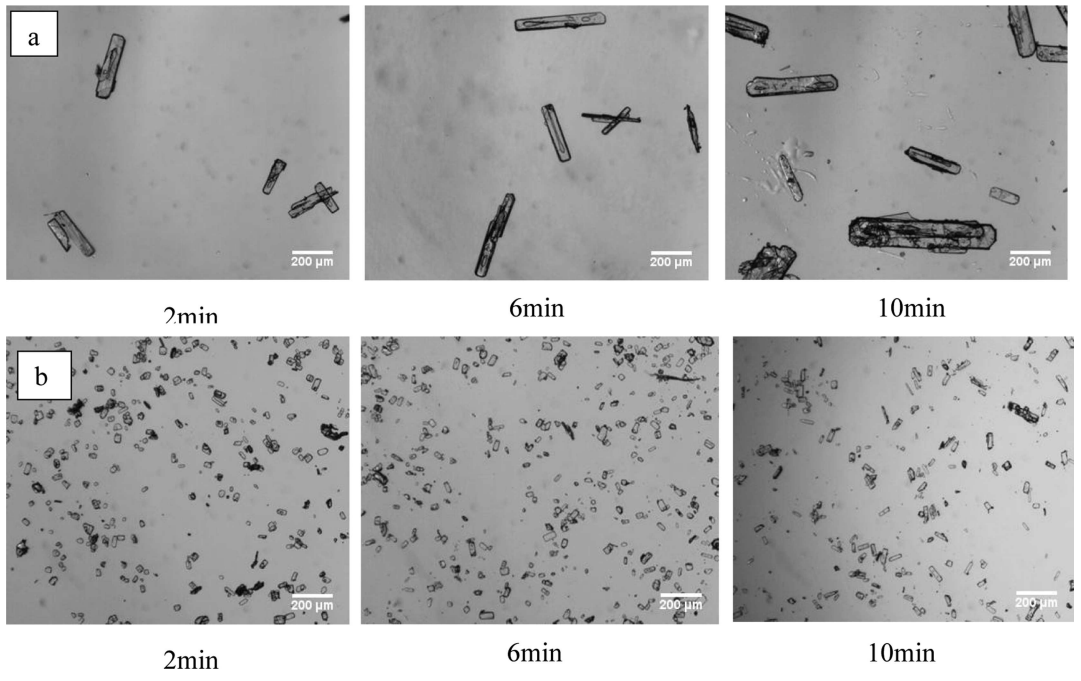

Figure 10. Variation in crystal size with respect to time (a) at 400 rpm of stirring speed, and (b) at 40% amp power of ultrasound.

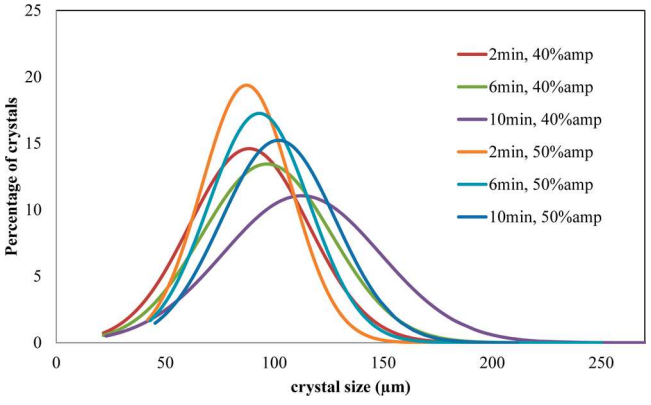

Figure 11. Increase in crystal size with respect to time at 40% and 50% amp of ultrasound at 0.018 mL/s of addition rate.

entire volume will be faster due to the ultrasonic action, and hence the precipitated benzoic acid readily forms new nuclei and some of the compound reaches the surface of the crystals due to mass transfer of solute to the surface of the formed nuclei resulting in subsequent growth. Also, the turbulence generated by the cavitating conditions results in the possible attrition and breakage effects for the crystals, and hence a lower mean size will be observed. Ultrasound also increases the bulk phase mass transfer[24] resulting in the enhancement in the growth rate. It is important to note here that the effect of ultrasound on growth rate will be lower as compared to the effect on nucleation rate and the particle breakage especially at higher power levels, and hence lower mean size is observed.

4.6. Effect of Antisolvent Addition Rate on the Crystal Size. Experiments were carried out with varying antisolvent addition rate (Q) over the range of 0.018−0.1 mL/s adjusted by changing the rpm of the peristaltic pump. Addition rate of antisolvent affects the crystal size, MSZW, and induction time for the formation of nuclei. As the flow rate increases, it has been observed that the induction time decreased and MSZW increased. Induction time decreases because of the creation of high local supersaturation and is also attributed to the fact that solution is reaching MSZW rapidly to form the nuclei. It has been observed that the crystal size of benzoic acid crystals decreased with increasing antisolvent addition rate as shown in Figure 12 for the conventional crystallization. This may be due

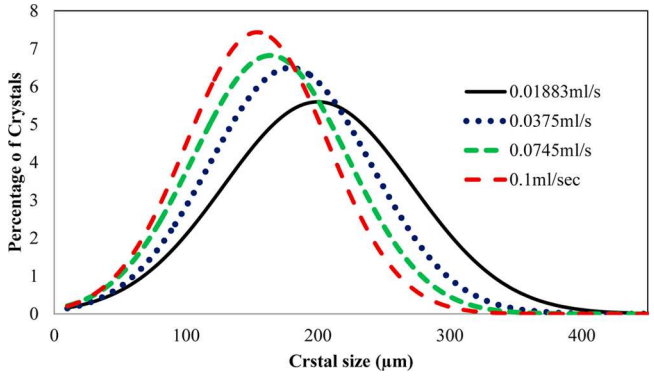

Figure 12. Effect of antisolvent addition rate on crystal size at 400 rpm of stirring and 0.4 kg/kg of concentration.

to the formation of more nuclei with an increase in antisolvent addition rate. This behavior of decrease in crystal size was observed in both cases of conventional and ultrasonic crystallization. A similar result of decrease in crystal size with respect to addition rate of antisolvent has been reported for the benzophenone crystals produced by the addition of water.[33]

For the case of ultrasonication, it has been observed that antisolvent addition rate affects the crystal size to a higher degree, and as the addition rate increases, crystal size distribution becomes narrow. At the addition rate of 0.018 mL/s, population density of the benzoic acid crystals was predicted by simulation as shown in Figure 13. The mean crystal size is around 80 μm. The result of population balance simulation matched the experimental observation of ultrasonic

dx.doi.org/10.1021/ie402203k | Ind. Eng. Chem. Res. 2013, 52, 17573−17582

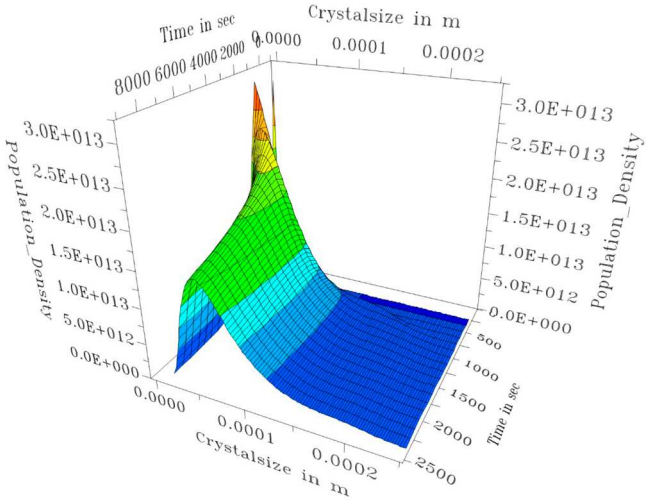

Figure 13. Predicted population balance for the ultrasonic antisolvent crystallization at 50% amp and 0.1 mL/s addition rate at $k_g = 2 \times 10^{-8}$, $k_b = 2.3 \times 10^9$.

crystallization with respect to crystal size. It has been observed that simulation does not show any nuclei in terms of population density for a particular time as the process of converting liquid from unsaturated to saturated state decides the nucleation. Later, this mean population density decreased due to the increase in crystal size to give a broader distribution of crystals. The observed variation in the effects of ultrasonic-assisted approach and the conventional approach can be possibly attributed to the types of flow and turbulence generated in the two cases. It is expected that conventional stirring results in dominant macroscopic mixing effects, whereas in the case of ultrasound, dominant microscopic level effects in terms of liquid circulation and turbulence are observed. It is important to note here that more work is required in this direction in terms of exactly analyzing the mixing effects due to the two modes of energy dissipation, which is out of the current scope.

5. CONCLUSIONS

The process of antisolvent crystallization of benzoic acid has been studied under varying parameters of ultrasound, agitation speed of stirrer, and addition rate of antisolvent. Ultrasonic crystallization has been observed to be a more efficient process to produce fine crystals of benzoic acid with high purity and morphology. An increase in the ultrasound power gives a narrow crystal size distribution, but higher power dissipation required additional cooling to control the temperature of the process. There is a mixed effect of agitation on the crystal size, and higher agitation rates resulted in bigger crystals, whereas lower agitation rate produced more agglomerates. Higher addition rates of antisolvent gave smaller crystal size. The combination of higher antisolvent addition rate and ultrasound gives very small crystals of high purity and shape. Kinetics of antisolvent crystallization of benzoic acid has been established by measuring the crystal size with respect to time. The mean crystal size of 80 μm has been obtained in the case of sonication, whereas a higher mean crystal size of 340 μm has been found in the conventional stirring process. It has been concluded that the growth rate and nucleation rate parameters are important in modeling of antisolvent crystallization, and the inclusion results in better matching with the experimental results as confirmed in the present work.

AUTHOR INFORMATION

Corresponding Author

*Phone: 022 33612024. Fax: 022 33611020. E-mail: pr.gogate@ictmumbai.edu.in.

Notes

The authors declare no competing financial interest.

NOMENCLATURE

B = nucleation rate [number/m^3/s]
b = nucleation order
C = concentration of the solute [kg/kg]
C^* = equilibrium concentration of solute [kg/kg]
G = growth rate [m/s]
g = growth order
i = empirical parameter
k_b = nucleation rate coefficient [number/m^3·s]
k_g = growth coefficient [m/s]
k_v = Shape factor
L = characteristic length of crystal [m]
M = magma density of the crystals [kg/kg]
m_T = total mass of mother liquor [kg]
m_s = mass of solid phase [kg]
m_l = mass of liquid phase [kg]
$m_{solvent}$ = mass of solvent initially added [kg]
n = population density [number/m^3]
Q = antisolvent flow rate [m^3/s]
t = crystallization time [s]
x = fraction of antisolvent in total mass of liquid

Greek Letters

ρ_c = density of the liquid [kg/m^3]
σ = supersaturation ratio (dimensionless)

REFERENCES

(1) Mersmann, A. *Crystallization Technology Handbook*; CRC Press: New York, 2001; pp 1−2144.
(2) Myerson, A. S.; Anderson, S. R.; Bennett, R. C.; Green, D.; Karpinski, P. *Handbook of Industrial Crystallization Contributors*; Butterworth-Heinemann: Woburn, MA, 2001.
(3) Kim, K. J.; Kim, J. K. Nucleation and supersaturation in drowning-out crystallization using a T-mixer. *Chem. Eng. Technol.* **2006**, *29*, 951−956.
(4) Zijlema, T. G.; Geertman, R. M.; Witkamp, G. J.; Van Rosmalen, G. M.; De Graauw, J. Antisolvent crystallization as an alternative to evaporative crystallization for the production of sodium chloride. *Ind. Eng. Chem. Res.* **2000**, *39*, 1330−1337.
(5) Jafari, D.; Nowee, S. M.; Noie, S. H. The prediction of thermodynamic-kinetic behavior of anti solvent crystallization from sodium chloride aqueous systems containing non-electrolytes. *Int. J. Appl. Sci. Eng. Res.* **2012**, *1*, 312−326.
(6) Ciardha, C. T. O.; Hutton, K. W.; Mitchell, N. A.; Frawley, P. J. Simultaneous parameter estimation and optimization of a seeded antisolvent crystallization. *Cryst. Growth Des.* **2012**, *12*, 5247−5261.
(7) Ciardha, C. T. O.; Frawley, P. J.; Mitchell, N. A. Estimation of the nucleation kinetics for the anti-solvent crystallisation of paracetamol in methanol/water solutions. *J. Cryst. Growth* **2011**, *328*, 50−57.
(8) Park, M.; Yeo, S. Anti-solvent crystallization of roxithromycin and the effect of ultrasound. *Sep. Sci. Technol.* **2010**, *45*, 1402−1410.
(9) Nagy, Z. K.; Fujiwara, M.; Braatz, R. D. Modelling and control of combined cooling and antisolvent crystallization processes. *J. Process Control* **2008**, *18*, 856−864.
(10) Lindenberg, C.; Krattli, M.; Cornel, J.; Mazzotti, M. Design and optimization of a combined cooling/antisolvent crystallization process. *Cryst. Growth Des.* **2009**, *9*, 1124−1136.

(11) Ruecroft, G.; Hipkiss, D.; Ly, T.; Maxted, N.; Cains, P. W. Sonocrystallization: The use of ultrasound for improved industrial crystallization. *Org. Process Res. Dev.* **2005**, *9*, 923−932.
(12) Sutkar, V. S.; Gogate, P. R. Design aspects of sonochemical reactors: Techniques for understanding cavitational activity distribution and effect of operating parameters. *Chem. Eng. J.* **2009**, *155*, 26−36.
(13) Gracin, S.; Uusi-penttila, M.; Rasmuson, Å. C. Influence of ultrasound on the nucleation of polymorphs of p-aminobenzoic acid. *Cryst. Growth Des.* **2005**, *5*, 1787−1794.
(14) Bucar, D.-K.; Macgillivray, L. R. Preparation and reactivity of nanocrystalline cocrystals formed via sonocrystallization. *J. Am. Chem. Soc.* **2007**, *2007*, 32−3.
(15) Li, H.; Li, H.; Guo, Z.; Liu, Y. The application of power ultrasound to reaction crystallization. *Ultrason. Sonochem.* **2006**, *13*, 359−63.
(16) Sivabalan, R.; Gore, G. M.; Nair, U. R.; Saikia, A.; Venugopalan, S.; Gandhe, B. R. Study on ultrasound assisted precipitation of CL-20 and its effect on morphology and sensitivity. *J. Hazard. Mater.* **2007**, *139*, 199−203.
(17) Ruecroft, G.; Hipkiss, D.; Ly, T.; Maxted, N.; Cains, P. W. Sonocrystallization: The use of ultrasound for improved industrial crystallization. *Org. Process Res. Dev.* **2005**, *9*, 923−932.
(18) Ramisetty, K. A.; Pandit, A. B.; Gogate, P. R. Investigations into ultrasound induced atomization. *Ultrason. Sonochem.* **2013**, *20*, 254−264.
(19) Nowee, S. M.; Abbas, A.; Romagnoli, J. A. Model-based optimal strategies for controlling particle size in antisolvent crystallization operations. *Cryst. Growth Des.* **2008**, *8*, 2698−2706.
(20) Stihl, M.; Bengt, L.; Rasmuson, C. Reaction crystallization kinetics of benzoic acid. *AIChE J.* **2001**, *47*, 1544−1560.
(21) Nowee, S. M.; Abbas, A.; Romagnoli, J. A. Antisolvent crystallization: Model identification, experimental validation and dynamic simulation. *Chem. Eng. Sci.* **2008**, *63*, 5457−5467.
(22) Katta, J.; Rasmuson, A. C. Spherical crystallization of benzoic acid. *Int. J. Pharm.* **2008**, *348*, 61−9.
(23) Shaikh, L.; Pandit, A.; Ranade, V. Crystallisation of ferrous sulphate heptahydrate: Experiments and modelling. *Can. J. Chem. Eng.* **2013**, *91*, 47−53.
(24) Luque de Castro, M. D.; Priego-Capote, F. Ultrasound-assisted crystallization (sonocrystallization). *Ultrason. Sonochem.* **2007**, *14*, 717−24.
(25) O'Grady, D.; Barrett, M.; Casey, E.; Glennon, B. The effect of mixing on the metastable zone width and nucleation kinetics in the anti-solvent crystallization of benzoic acid. *Chem. Eng. Res. Des.* **2007**, *85*, 945−952.
(26) Barrett, M.; O'Grady, D.; Casey, E.; Glennon, B. The role of meso-mixing in anti-solvent crystallization processes. *Chem. Eng. Sci.* **2011**, *66*, 2523−2534.
(27) Lin, C.; Muhrer, G.; Mazzotti, M.; Subramaniam, B. Vapor−liquid mass transfer during gas antisolvent recrystallization: Modeling and experiments. *Ind. Eng. Chem. Res.* **2003**, *42*, 2171−2182.
(28) Torbacke, M.; Rasmuson, Å. C. Mesomixing in semi-batch reaction crystallization and influence of reactor size. *AIChE J.* **2004**, *50*, 3107−3119.
(29) Chang, S.; Kim, J.; Kim, I.; Shin, D.; Kim, W. Agglomeration control of L-ornithine aspartate crystals by operating variables in drowning-out crystallization. *Ind. Eng. Chem. Res.* **2006**, *45*, 1631−1635.
(30) Plasari, E.; Grisoni, P. H.; Villermaux, J. Influence of process parameters on the precipitation of organic nanoparticles by drowning-out. *Chem. Eng. Res. Des.* **1997**, *75*, 237−244.
(31) Schmidt, C.; Yürüdü, C.; Wachsmuth, A.; Ulrich, J. Modeling the morphology of benzoic acid crystals grown from aqueous solution. *CrystEngComm* **2011**, *13*, 1159−1169.
(32) Park, M. W.; Yeo, S. D. Antisolvent crystallization of carbamazepine from organic solutions. *Chem. Eng. Res. Des.* **2012**, *90*, 2202−2208.
(33) Borissova, A.; Dashova, Z.; Lai, X.; Roberts, K. J. Examination of the semi-batch crystallization of benzophenone from saturated methanol solution via aqueous antisolvent drowning-out as monitored 2004. *Cryst. Growth Des.* **2004**, *4*, 1053−1060.